8

Laser Scanning Cytometry

Principles and Applications

Piotr Pozarowski, Elena Holden, and Zbigniew Darzynkiewicz

Summary

The laser scanning cytometer (LSC) is the microscope-based cytofluorometer that offers a plethora of analytical capabilities. Multilaser-excited fluorescence emitted from individual cells is measured at several wavelength ranges, rapidly (up to 5000 cells/min), with high sensitivity and accuracy. The following applications of LSC are reviewed: (1) identification of cells that differ in degree of chromatin condensation (e.g., mitotic or apoptotic cells or lymphocytes vs granulocytes vs monocytes); (2) detection of translocation between cytoplasm vs nucleus or nucleoplasm vs nucleolus of regulatory molecules such as NF-κB, p53, or Bax; (3) semiautomatic scoring of micronuclei in mutagenicity assays; (4) analysis of fluorescence *in situ* hybridization; (5) enumeration and morphometry of nucleoli; (6) analysis of phenotype of progeny of individual cells in clonogenicity assay; (7) cell immunophenotyping; (8) visual examination, imaging, or sequential analysis of the cells measured earlier upon their relocation, using different probes; (9) *in situ* enzyme kinetics and other time-resolved processes; (10) analysis of tissue section architecture; (11) application for hypocellular samples (needle aspirate, spinal fluid, etc.); (12) other clinical applications. Advantages and limitations of LSC are discussed and compared with flow cytometry.

Key Words: Cytometry; fluorescence; cell cycle; apoptosis; nucleus; nucleolus; micronucleus cytoplasm; enzyme kinetics

1. Introduction: Limitations of Flow Cytometry

During the past three decades, flow cytometry (FC)/cell sorting has become commonplace in various disciplines of biology, medicine, and biotechnology. However, because cells are measured while suspended in a stream of liquid and often discarded following the measurement, the analytical capability of FC is limited for many applications, such as the following:

1. Time-resolved events such as enzyme kinetics, drug uptake, or drug efflux cannot be analyzed on individual cells.

From: *Methods in Molecular Biology, vol. 319: Cell Imaging Techniques: Methods and Protocols*
Edited by: D. J. Taatjes and B. T. Mossman © Humana Press Inc., Totowa, NJ

2. The morphology of the measured cell might only be assessed after sorting, which is cumbersome and not always available.
3. Subcellular localization of the fluorochrome cannot be analyzed.
4. The cell once measured cannot be reanalyzed with another probe(s).
5. Analysis of solid tissue requires cell or nucleus isolation that leads to loss of information on tissue architecture.
6. Small-size samples such as fine-needle aspirates or spinal fluid are seldom analyzed by FC because repeated sample centrifugations, which often are required, lead to cell loss that has to be compensated for by starting with a large number of cells per sample.
7. The measured sample is lost and cannot be stored for archival preservation.

The microscope-based laser scanning cytometer (LSC), manufactured since the mid-1990s by CompuCyte Corp. (Cambridge, MA), offers many advantages of FC but has none of the limitations presented above. The analytical capabilities of LSC, therefore, complement those of FC and extend the use of cytometry in many applications *(1–4)*. This chapter is primarily focused on the applications and capabilities of LSC that are unique to this instrumentation and it updates the previous reviews *(4,5)*. Clinical applications of LSC were also recently reviewed *(6)*, as well as the applications of LSC in toxipathology *(7)*. A separate review that is focused on applications of LSC and other laser-based technologies in cell signaling in environmental lung disease was also recently published *(8)*.

2. Features of LSC and Parameters That Can Be Measured

The microscope (Olympus Optical Co.) is the key part of the instrument, and it provides essential structural and optical components (*see* **Fig. 1**). The beams from two or three lasers (argon ion and helium–neon; violet laser is optional) spatially merged by dichroic mirrors are directed onto the computer-controlled oscillating (350 Hz) mirror, which reflects them through the epi-illumination port of the microscope and images through the objective lens onto the slide. The mirror oscillations cause the laser beams to sweep the area of microscope slide under the lens. The beam spot size varies depending on the lens magnification, from 2.5 (at 40×) to 10.0 μm (at 10×). The slide, with its *xy* position monitored by sensors, is placed on the computer-controlled motorized microscope stage, which moves at 0.5-μm steps per each laser scan, perpendicular to the scan. Laser light scattered by the cells is imaged by the condenser lens and its intensity is recorded by sensors. The specimen-emitted fluorescence is collected by the objective lens and directed to the scanning mirror. Upon reflection, it passes through a series of dichroic mirrors and optical emission filters to reach one of the four photomultipliers. Each photomultipler records fluorescence at a specific wavelength range, defined by the combination of filters and dichroic mirrors. A light source, additional to the lasers, provides

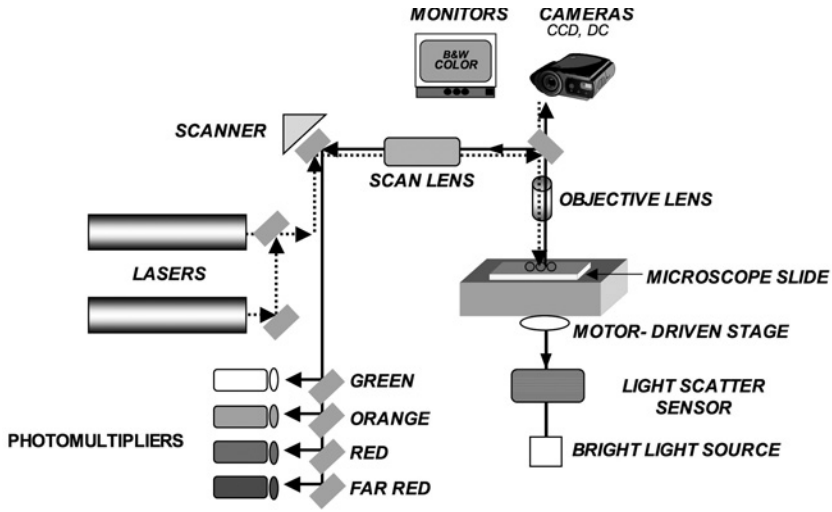

Fig. 1. Schematic representation of the LSC. *See* text for explanation.

transmitted illumination to visualize the objects through an eyepiece or the charge-coupled device (CCD) camera.

The measurement of cell fluorescence (or light scatter) is computer controlled and triggered by a threshold contour set above the background (*see* **Fig. 2**). The following parameters are recorded by LSC for each measured cell/object:

1. *Integrated fluorescence* intensity, representing the sum of intensities of all pixels ("picture elements") within the integration contour area. The latter can be adjusted to a desired width with respect to the threshold contour (*see* **Fig. 2**).
2. The maximal intensity of an individual pixel within this area (*maximal pixel;* "max pixel").
3. The *integration area*, representing the number of pixels within the integration contour.
4. The *perimeter* of the integration contour (in micrometers).
5. The fluorescence intensity integrated over the area of a torus of desired width defined by the *peripheral contour* located around (outside) the primary integration contour. For example, if the integration contour is set for the nucleus, based on red fluorescence (DNA stained by propidium iodide [PI]), then the integrated (or maximal pixel) green fluorescence of fluorescein isothiocyanate (FITC)- stained cytoplasm can be measured separately, within the integration contour (i.e., over the nucleus) and within the peripheral contour (i.e., over the rim of cytoplasm of desired width outside the nucleus). All of the above values of fluorescence (parameters 1, 2, and 5) are automatically corrected for background, which is measured outside the cell, within the *background contour* (*see* **Fig. 2**).

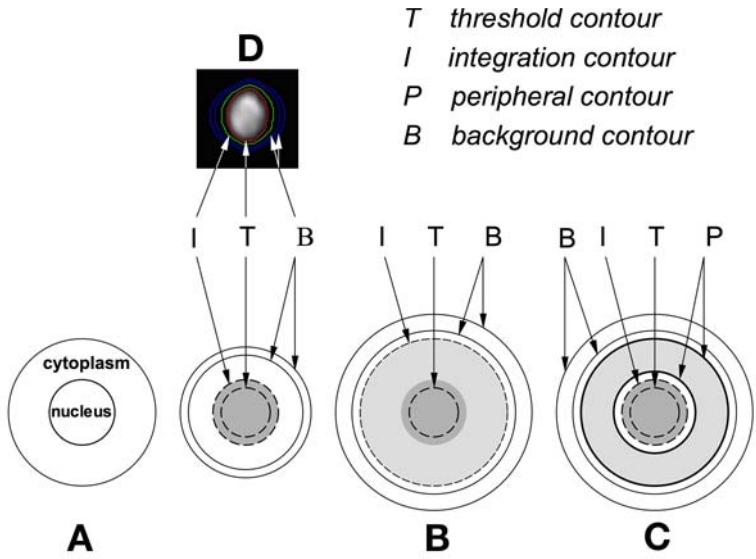

Fig. 2. Different settings for analysis of nuclear, total, and/or cytoplasmic fluorescence by LSC. When nuclear DNA is stained with a red fluorescing dye (e.g., propidium), the threshold contour (T) is set on the red signal to detect the nucleus **(A)**. The integration contour (I) is then set a few pixels outside of T to ensure that all nuclear fluorescence is measured and integrated **(A)**. However, when cytoplasmic fluorescence also is measured, I is set far away from T to ensure that fluorescence emitted from the cytoplasm is integrated as well **(B)**. It also is possible to separately measure nuclear and cytoplasmic fluorescence, as shown in **(C)**. The peripheral contours (P) are then set at the desired number of pixels outside of I and the fluorescence intensities emitted from both areas (viz. within the I boundary and within the P torus) are separately measured and separately integrated. In each case, the background contour is automatically set outside the cell, and the background fluorescence is subtracted from nuclear, cytoplasmic, or total cell fluorescence. The actual cell's contours, as they appear on the monitor, are shown in **(D)**.

6. The *xy* coordinates of maximal pixel locating the measured object on the microscope stage.
7. The computer clock *time* at the moment of measurement.

The software of LSC (WinCyte) allows one to obtain ratios of the respective parameters as a new parameter, and the ratiometric data can be displayed during data analysis. The electronic compensation of fluorescence emission spectral overlap is one of the features of the data analysis. The compensation at the time of data analysis is more convenient than in real time, as it is in most flow cytometers, because it provides an opportunity to test and compare different settings for optimal results.

In addition to the above-listed parameters, the WinCyte software of LSC is also designed to analyze the fluorescence *in situ* hybridization (FISH). Toward this end, the software allows one to establish, within a primary contour representing a nucleus stained with a particular dye (e.g., propidium), a *second set of contours* representing another color (e.g., FITC) fluorescence. Five secondary features are then measured in addition to the major features that were listed above, namely (1) number of secondary contours (i.e., FISH spots); (2) distance between the nearest spots; (3) integrated fluorescence; (4) maximal pixel fluorescence, as well as (5) fluorescence area. The last three parameters (3–5) are measured for each secondary contour.

The measurements by LSC are relatively rapid; having optimal cell density on the slide, up to 5000 cells can be measured per minute. The accuracy and sensitivity of cell fluorescence measurements by LSC are comparable to the advanced flow cytometers ***(1,2)***.

Another methodology that can be utilized to quantify cell constituents measuring fluorescence, in addition to LSC and FC, is fluorescence image analysis (FIA). In FIA, the cell illumination is uniform, provided by a mercury or xenon arc epi-illuminator. A bandpass filter selects fluorescence of a desired wavelength that is imaged at a low depth of focus by a CCD camera. Compared with LSC or FC that utilize photomultipliers, the dynamic range of sensitivity of fluorescence intensity measurement by a CCD is lower in FIA. FIA, thus, cannot provide quantitative analysis of fluorescence intensity that would be on par with FC or LSC. The image, however, can be analyzed by FIA at higher spatial resolution than by LSC.

3. Maximal Pixel of Fluorescence Intensity

Maximal pixel of fluorescence intensity (MPFI) is a useful reporter of local intracellular hypochromicity or hyperchromicity, reflecting a low or high concentration (density) of the fluorescent probe in intracellular compartments. One of the early applications of LSC along this line was to identify cells with condensed chromatin; namely, because DNA in condensed chromatin, such as of mitotic or apoptotic cells, shows increased staining intensity (per unit area of chromatin image, because the same amount of chromatin is compacted at a higher spatial density) with most fluorochromes, the MPFI of these cells is higher than that of cells with the same DNA content but with diffuse chromatin ***(9,10)***. Although mitotic cells can be recognized by FC using a variety of markers (reviewed in **ref.** ***11***), the advantage of the MPFI approach is that a single fluorochrome is used to distinguish G_1 vs S vs G_2 vs M phase cells. It is possible, thus, to use another color fluorochrome(s) to detect other cell constituents instead of to identify M cells. This approach was used to combine pulse labeling of DNA replicating cells with bromodeoxyuridine (BrdU) (detected with

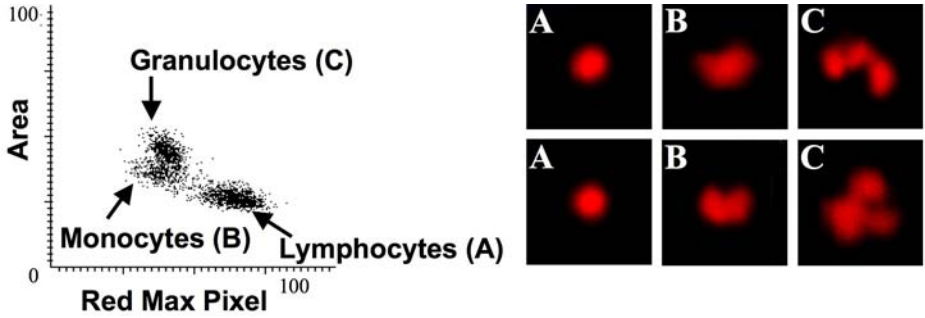

Fig. 3. Distinction of granulocytes, monocytes, and lymphocytes by LSC based on differences in their area vs maximal pixel of red fluorescence, after staining with propidium iodide (*20*).

anti-BrdU mAb) with the identification of mitotic cells to study the cell cycle kinetics by the fraction of labeled mitoses (FLM) method *(12)*. The FLM assay, initially designed for tritiated thymidine autoradiography *(13)*, yields a wealth of information on cell cycle kinetics but is cumbersome and time-consuming. Its adaptation to LSC simplifies the procedure and shortens the time of analysis *(12)*. Similar to mitotic chromosomes *(8)*, BrdU-labeled meiotic chromosomes were identified by LSC in studies of mutagenesis *(14)*.

Apoptotic cells having condensed chromatin *(15,16)* also can be identified by MPFI of DNA-associated fluorescence *(17,18)*. It should be cautioned, however, that because both mitotic and apoptotic cells are characterized by a high value of MPFI, the distinction of G_2/M apoptotic cells from mitotic cells is not always possible by this method. This limitation is of particular importance when apoptosis is induced by agents that arrest cells in mitosis and, therefore, the sample contains mitotic cells that die by apoptosis. MPFI has also been found useful to detect localized caspase activity in early apoptotic cells by analysis of local intracellular accumulation of the caspase-cleavage product of the fluorogenic substrate *(19)*.

The MPFI of DNA-associated fluorescence can also be used to distinguish lymphocytes from monocytes and from granulocytes, the cell types that differ by the degree of chromatin condensation (*see* **Fig. 3**). The fluorescence area, the parameter that reflects nuclear size and is correlated (inversely) with chromatin condensation, also is different for lymphocytes, monocytes, and granulocytes *(20)*.

Translocation of macromolecules to different subcellular compartments *if it is associated with a change in their local density* (concentration) can also be traced by the measurement of the changes of MPFI. For example, translocation of the proapoptotic regulatory protein Bax and its accumulation in mitochondria, the event that facilitates release of cytochrome-*c* and activation of caspases *(21,22)*,

is detected by LSC as an increase in MPFI of Bax immunofluorescence *(23)*. The analysis of MPFI to detect translocation of other macromolecules might find other applications (e.g., to monitor activation or deactivation of the signal transduction proteins, receptor clustering, accumulation of protein in the Golgi apparatus, etc.).

4. Nuclear vs Cytoplasmic Localization of Fluorescence

Most cellular DNA is localized in the nucleus (the content of mitochondrial DNA is minimal); therefore when DNA is fluorochrome stained, it provides a good marker defining the nuclear boundary. If another color fluorochrome is used to mark other cell constituents, LSC is then able to resolve and separately measure the nuclear and cytoplasmic content of this constituent (*see* **Fig. 2**). This capability can be used to detect translocation of particular proteins from cytoplasm to nucleus, or vice versa (e.g., to monitor the traffic of signal transduction or activation molecules). A classical example of such a protein is nuclear factor kappa B (NF-κB). This ubiquitous factor is involved in regulation of diverse immune and inflammatory responses and also plays a role in the control of cell growth and apoptosis *(24)*. Inactive NF-κB remains in the cytoplasm bound to I-κB protein. Rapid translocation of NF-κB from cytoplasm to the nucleus occurs in response to extracellular signals or DNA damage and is considered to be a hallmark of activation *(24)*. NF-κB was detected immunocytochemically in several leukemic cell lines with FITC-tagged antibody, and its presence in the nucleus vis-a-vis cytoplasm was monitored by LSC measurements of green fluorescence (FITC) integrated over the nucleus vs over the cytoplasm *(25)*. Activation led to a rapid increase in NF-κB-associated fluorescence measured over the nucleus concomitant with a decrease in fluorescence over the cytoplasm, which was reflected by a large increase in the nuclear-to-cytoplasmic fluorescence ratio (*see* **Fig. 4**). One of the virtues of this assay is that NF-κB activation could be correlated with cell morphology, immunophenotype, or cell cycle position *(25)*. The assay of NF-κB translocation by LSC has been found more sensitive than by either of the four alternative methods *(26)*. This application of LSC can be extended to monitor other factors that, upon activation, accumulate in cytoplasm and/or undergo translocation to the nucleus, such as tumor suppressor p53 and signal transduction or cell cycle regulatory molecules. Indeed, the upregulation and translocation of p53 from cytoplasm to the nucleus in response to DNA damage by the topoisomerase I inhibitor camptothecin, detected by LSC, was recently reported *(27)*.

The possibility of measurement of only nuclear-associated fraction of proliferating cell nuclear antigen (PCNA) detected immunocytochemically as offered by LSC provided a good distinction of the S-phase cells in histopathological analysis of renal cell carcinoma *(28)*.

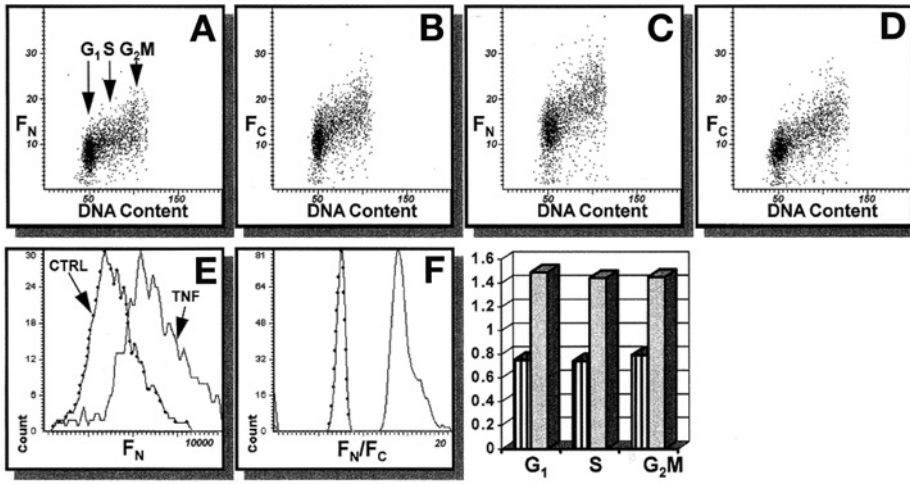

Fig. 4. Changes in intensity of NF-κB immunofluorescence integrated over the cell nucleus (F_N) **(A,C)** and cytoplasm (F_C) **(B,D)** of the U-937 histiomonocytic lymphoma cells, untreated (**A,B**) and treated for 1 h with 10 ng/mL of tumor necrosis factor (TNF)-α **(C,D)**. Note the increase in F_N after the treatment **(E)** and even more pronounced increase in the F_N/F_C ratio **(F)**. Bars indicate F_N/F_C of the cells gated in G_1, S, and G_2/M based on differences in their DNA content as shown in **(A)**; striped bars, prior to TNF-α treatment; shaded bars, after the treatment *(25)*.

It should be stressed, however, that in the case of highly asymmetrically shaped cells (e.g., fibroblasts, neurons) or cells with acentric position of the nucleus (e.g., muscle cells) that grow on slides, the integration of fluorescence from the entire cytoplasm is problematic. A partial solution to the problem might be cell trypsinization followed by their deposition on slides by cytocentrifugation. The cells that grow asymmetrically then become more spherical, with the nucleus centrally located.

5. The Micronucleus Assay/Genotoxicity Studies

The micronucleus assay is widely used to assess the chromosomal or mitotic spindle damage induced by ionizing radiation or mutagenic agents in vivo or in vitro. Because visual scoring of micronuclei is cumbersome, semiautomatic procedures that rely either on flow cytometry or image analysis were developed. The classic image analysis, however, appears to be a complex approach and its practical utility to quantify frequency of micronucleation has been limited to relatively few laboratories with proper expertise and instrumentation. LSC was recently adapted for the analysis of micronucleation induced by genotoxic agents in vivo in mouse erythrocytes *(29)* as well as in vitro in cultured cells *(30)*. The capability of LSC to relocate micronuclei for visual

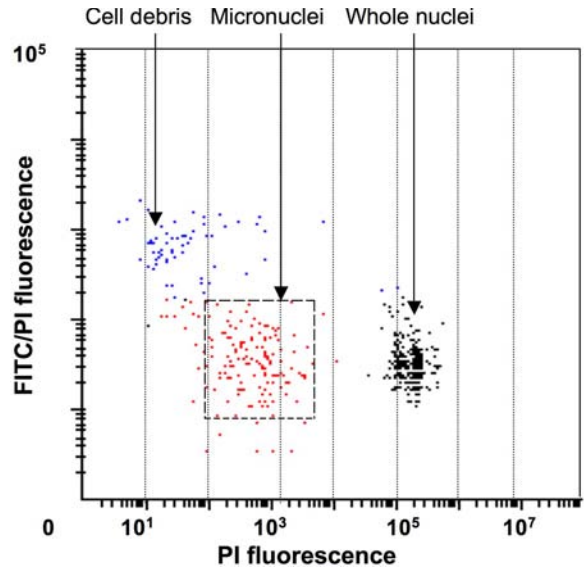

Fig. 5. Detection of micronuclei by LSC. To induce micronuclei, HL-60 cells were treated with mitomycin C, then cytocentrifuged, fixed, and stained with FITC and PI. Micronuclei (located on this scatterplot within the dashed-line gating window where approx 93% of all the events occur) were identified by their low DNA content (PI fluorescence) ranging between 0.1% and 5% of that of the whole G_1 nuclei and the FITC/PI fluorescence ratio that was similar to that of the whole nuclei ***(30)***.

examination was useful to confirm their identification. Multiparameter characterization of micronuclei that took into account their DNA content and protein/DNA ratio (*see* **Fig. 5**) made it possible to establish the gating parameters that excluded objects that were not micronuclei ***(30)***. The percentage of micronuclei assayed by LSC correlated well with that estimated visually by microscopy in both studies ***(29,30)***. LSC, thus, can be used to obtain an unbiased estimate of frequency of micronuclei more rapidly than by conventional examination of the preparations by microscopy. Additionally, unlike flow cytometry, LSC allows one to characterize individual cells with respect to frequency and DNA content of micronuclei in these cells. Furthermore, it can be applied to the cytokinesis-blocked (e.g., by cytocholasin B) micronuclei assay ***(30)***. These analytical capabilities of LSC might be helpful not only to score micronuclei but also to study mechanisms of induction of micronuclei by clastogens or aneugens through their effects on chromosomes or mitotic spindles, respectively.

Assessment of DNA damage is another measure of genotoxicity or can be used as a marker of cell death (apoptosis). LSC has found an application for this

purpose as well, specifically for measuring the extent of DNA electrophoretic mobility from individual cells in the "comet" *(31)* or "halo" *(32)* assays.

6. Applications of LSC Utilizing the WinCyte Software Designed for FISH Analysis

6.1. FISH Analysis, Cytogenetic Studies

The semiautomated FISH analysis represents still another LSC application that is based on its ability to spatially resolve the distribution of fluorescent regions within the cell *(2,33)*. As mentioned, the software developed for this application allows one to establish, within a primary contour representing, for example, nucleus stained with a particular dye (e.g., propidium), a second set of contours representing another color (e.g., FITC) fluorescence. An obvious advantage of LSC over visual analysis of FISH is the unbiased selection of the measured cells and their semiautomated, rapid measurement. Furthermore, analysis of the integrated fluorescence intensity of the secondary contours might yield information pertaining to the degree of amplification of particular genome sections. Thus, for example, Kobayashi et al. *(34)*, using the dual color FISH analysis by LSC, revealed an increase in 20q13 chromosomal copy number in several breast cancer cases and correlated it with DNA ploidy and estrogen receptor (ER) or progesterone receptor status. LSC has also found utility in studies employing comparative genomic hybridization (CGH) to reveal cytogenetic aberrations in several types of human cancer *(35–37)* or in studies of DNA ploidy in sperm cells *(38)*. It should be noted, however, that semiautomated FISH measurements by LSC require high-quality technical preparations *(2,33)*.

6.2. Analysis of Nucleoli and Protein Translocations Between Nucleoli and Nucleoplasm

The capacity of the LSC software originally designed for semiautomatic FISH analysis can be applied to other applications. One such application is quantitative analysis of nucleoli and monitoring traffic of molecules between nucleoli and nucleoplasm *(39,40)*. A useful immunocytochemical marker of nucleoli is an antibody to the nucleolar protein nucleolin. Using this antibody, it was possible to estimate the size of individual nucleoli (area and circumference), number of nucleoli per nucleus, total nucleolar area per nucleus, as well as expression of nucleolin separately in nucleoli and nucleoplasm (*see* **Fig. 6**). All of these parameters have been found to strongly correlate with the proliferative status and the cell cycle position of mitogenically stimulated lymphocytes *(40)*. Most interesting, however, was the observation that abundance of nucleolin in nucleoplasm was maximal during the cell transition from the G_0 to G_1 phase of the cycle, which corresponded to the maximal rate of rRNA synthesis

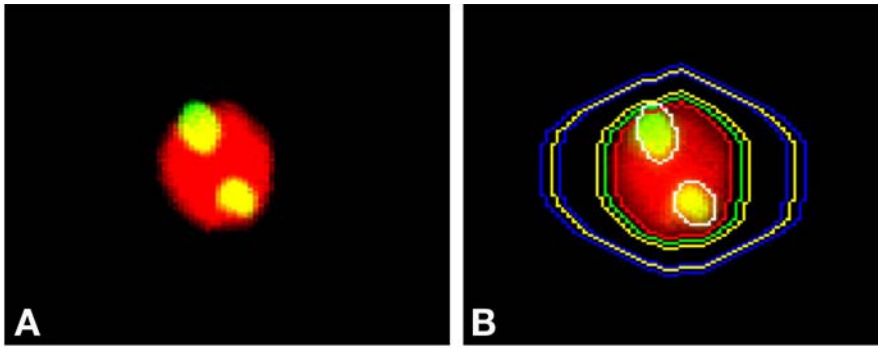

Fig. 6. Analysis of nucleoli in mitogen-stimulated lymphocytes. Nucleolin antibodies were used to immunostain nucleoli in 48 h-phytohemagglutinin-stimulated human lymphocytes; DNA was counterstained with propidium iodide. The software of LSC designed for FISH analysis was used to separately contour the cell nucleus and the nucleoli. The approach allows one to measure number of nucleoli, their size, expression of nucleolin in nucleoli and in nucleoplasm; all in relation to the cell cycle phase ***(40)***.

and its accumulation within the cell. The translocation of nucleolin from nucleoplasm to nucleoli was observed at later stages of lymphocyte stimulation, when the cells were progressing through G_1, S, and G_2/M and when the rate of rRNA accumulation was decreased ***(40)***. Similar application of LSC revealed the cell-cycle-phase-associated nucleoplasm–nucleolar shuttling of cyclin E, which was defective in bladder cancer cells ***(39)***.

6.3. Progeny of Individual Cells/Clonogenicity Assay

Another application of LSC utilizing FISH software was demonstrated in the analysis of progeny (clones) of individual cells ***(41)***. In this application, cellular protein and DNA have been stained with fluorochromes of different colors and the product of tumor suppressor gene *p53* or estrogen receptor was detected immunocytochemically, with still another color fluorescent dye. The threshold contour was set on protein-associated fluorescence, which made it possible to analyze the *whole-cell colony as a single entity* (*see* **Fig. 7**). This approach made it possible to measure a variety of attributes of the progeny of individual cells (phenotype of individual cell colonies), such as colony size (area, circumference, cell number per colony), DNA and protein content per colony, expression of *p53* or estrogen (per colony, per cell, per unit of DNA or protein), the colonies' heterogeneity, and the cell cycle distribution of individual cells within colonies. Such multiparameter analysis provided a wealth of information and was used to study mechanisms by which the cytotoxic RNase–onconase affected proliferative capacity of the cells and induced growth imbalance and

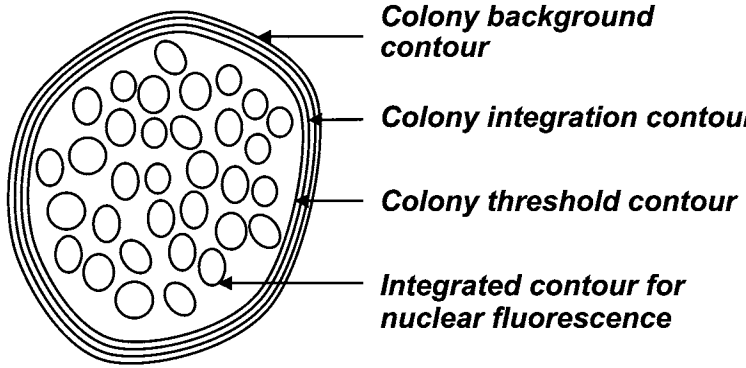

Fig. 7. Strategy used to analyze individual cell colonies by LSC. The MCF-7 breast cancer cell colonies growing on a microscope slide were fixed, and cellular DNA was stained with PI (excited by an argon-ion laser), total protein was stained with BODIPY 630/650X (excited by a neon–helium laser), and individual proteins (tumor suppressor *p53*, or estrogen receptor [ER]) were stained with FITC-tagged Ab (excited by an argon-ion laser). The colony threshold contour and integration contour were set based on BODIPY 620/650X fluorescence. It was possible to estimate total DNA content, content of total protein, and content of *p53* (or ER) per individual colony. Ratiometric analysis revealed ratios of total protein per DNA, *p53* per DNA, or ER per DNA, as well as *p53* (or ER) per total protein for each colony. Furthermore, it was possible to estimate the number of nuclei (cells) per colony and cell cycle distribution within each colony. Such multiparametric analysis of progeny of individual cells provided a sensitive assay to monitor not only the drug-induced changes in cell proliferation but also in their phenotype ***(41)***.

differentiation ***(41)***. Extensions of LSC might make this instrument applicable for automatic analysis of cloning efficiency and multiparameter analysis of cell colonies in soft agar. Such analyses might be useful in studies of mechanisms and effectiveness of antitumor drugs in the field of carcinogenesis and for analysis of primary cultures, assessing tumor prognosis and drug sensitivity. The assay can also be adapted to analysis of microbial colonies.

7. Cell Immunophenotyping

Laser scanning cytometry has been adapted to carry out routine immunophenotyping. Multichamber microscope slides were developed that can be used to automatically screen cells against up to 36 antibodies on a single slide by LSC ***(42–46)***. The chambers are filled with cell suspension by capillary action. In the absence of serum or other proteins in the suspension, the cells strongly attach to the floor of the chambers by electrostatic interactions ***(42,45)***. Various antibody combinations are then introduced into the chambers, the cells are incubated in

their presence for 30–60 min, and following a buffer rinse, their fluorescence is measured. The rate of analysis is relatively fast, as it takes approx 20 min to screen the cells distributed in 12 wells labeled with a panel of 36 antibodies (3 antibodies at a time) measuring 3000–5000 cells per well *(42)*.

Although the rate of measurement by LSC is slower than flow cytometry and the lack of side (90° angle) light-scatter analysis impedes discrimination of lymphocytes from monocytes and granulocytes, certain advantages of LSC might outweigh these deficiencies. Thus, LSC is preferred for hypocellular samples, which cannot tolerate repeated centrifugations that lead to cell loss. It has to be stressed that cell loss during centrifugations, as required for flow cytometry analysis, is not random but preferential to different cell types *(20)*. LSC is also economical: Because of the small sample size in LSC, the cost of the reagents (mAbs) is reduced by over 80% compared to flow cytometry *(34)*. Furthermore, LSC provides the possibility to relocate immunophenotyped cells for additional analysis or archival preservation (*see* **Subheading 8.**).

8. The Relocation Feature

8.1. Visual Cell Examination

Because the spatial *xy* position of the measured cell is recorded, it is possible to relocate such a cell for visual examination by microscopy or imaging. The possibility to subject the measured cells to morphological examination is particularly important in studies of apoptosis. This is because apoptosis was originally defined by morphological criteria *(47)* and cell morphology still remains the gold standard to identify this mode of cell death *(15,16)*. Using LSC, it was possible to discriminate between the genuine apoptotic cells and "false-positive" cells in peripheral blood and bone marrow of leukemic patients undergoing chemotherapy *(18)*. The latter cells were monocytes/macrophages containing apoptotic bodies (probably ingested from the disintegrating apoptotic cells) in their cytoplasm. Although both the genuine apoptotic cells and the "false-positive" cells contained numerous DNA strand breaks and were indistinguishable by FC, analysis of their morphology by LSC made their positive identification made possible *(18)*. In another study, the eosinophils were identified by LSC as "false-positive" apoptotic cells because of their nonspecific labeling with fluorescein-conjugated reagents *(48)*. LSC was also helpful to distinguish apoptotic cells from the cells infected by human granulocytic erlichiosis *(49)*. Based on these observations and other findings, it was concluded that LSC is the instrument of choice for the analysis of apoptosis *(18,50,51)*.

Several other methods of identification of apoptotic cells, including their recognition by the presence of DNA strand breaks, decreased mitochondrial transmembrane potential, cleavage of poly (ADP-ribose) polymerase, or fractional DNA content (reviewed in **refs.** *15* and *16*), have been successfully

adapted to LSC *(18,52–58)*. More recently, LSC was used to measure activation of caspases during apoptosis by the method utilizing fluorochrome-labeled caspase inhibitors (FLICA) *(58,59)*, activation of serine-proteases using a similar approach *(61)*, as well as to detect segregation of RNA from DNA and their separate packaging into apoptotic bodies *(62)*. In all of these studies, the possibility of cell relocation for visual assessment of apoptosis was a valuable feature of LSC.

The relocation feature of LSC was also useful for the "comet" (single-cell elecrophoresis) assay *(31)*. In this assay, the cells with damaged DNA were subjected to electrophoresis; then LSC was used to determine the DNA-associated fluorescence of the comets' heads (undamaged DNA), followed by image acquisition of each comet and digital image analysis and computation of tail (damaged DNA) moment and the head-DNA content measurement. A strong inverse correlation was observed between the tail moment and content of undamaged DNA *(31)*.

8.2. Sequential Analysis of the Same Cells With Different Probes

Laser scanning cytometry allows one to integrate the results of two or more measurements into a single file (the "file-merge" feature). This feature provides the opportunity to measure the same cells more than once, using different settings or probes. For example, it is possible to set the integration contour first on the nucleus and, subsequently, on the whole cell. This approach enables one to separately measure particular constituents in the nucleus and in the whole cell. Such analysis has been applied to reveal translocation of cyclin B1, detected immunocytochemically, from cytoplasm to nucleus during mitosis *(63)*.

Another application of the file-merge feature of LSC was recently described for analysis of cellular DNA and double-stranded (ds) RNA *(64)*. The cells were stained with propidium iodide (PI) and measured twice, prior to and after the incubation with RNase. The integrated value of PI intensity of individual cells during the first measurement was proportional to their DNA plus dsRNA content. The PI fluorescence intensity during the subsequent measurement was the result of the dye interaction with DNA only. Thus, when the second measurement was subtracted from the first measurement, the difference ("differential fluorescence" [DF]) represented the RNA-associated PI fluorescence only. DF was then used as a *separate parameter* that was recorded in list mode in the merged file. Cellular protein was also counterstained, but with a fluorochrome of another color of emission than PI. The multiparameter analysis of these data made it possible to correlate, within the same cells, the cellular ds RNA content with DNA content (cell cycle position) or with protein content *(64)*. This novel approach of using the DF as an additional, discrete parameter for the bivariate or multivariate analysis extends the application of LSC for bivariate or multivariate analysis

of other cell constituents, which might be differentially stained with the same wavelength of emission fluorochromes.

Still another application of the file-merge feature and sequential cell staining was to study, within the same cells, a correlation between the supravitally detected cell attributes such as mitochondrial transmembrane potential or induction of oxidative stress, with the attributes to be detected requiring cell fixation, such as the presence of DNA strand breaks or DNA content ***(65)***. This approach revealed that the loss of the transmembrane potential during apoptosis was either very transient or not correlated at all with the activation of caspases and DNA cleavage ***(66)***.

8.3. Enzyme Kinetics and Other Time-Resolved Events

The time of cell measurement by LSC is recorded in the list mode file together with other measured parameters. The relocation feature, in turn, makes it possible to measure the same cell repeatedly. LSC, unlike flow cytometry, thus provides the means to measure kinetic reactions within individual cells in large cell populations. Using the fluorogenic substrate di-(leucyl)-rhodamine 110, the kinetic activity of L-aminopeptidase was measured in several cell types by LSC ***(67)***. The rate of fluorescein di-acetate hydrolysis by esterases as well as the rate of uptake of the lysosomo-trophic fluorochrome acridine orange also was assayed ***(67)***. Several hundred cells per sample were measured with a time resolution of 10–60 s. The kinetic curves constructed for individual cells were matched with the respective cells; the latter were stained with conventional absorption dyes and following the relocation by LSC, they were identified as monocytes, granulocytes, or lymphocytes using bright-field illumination ***(67)***. In a similar manner, the kinetics of dissociation of fluorochromes from nuclear DNA, induced by caffeine, were measured by LSC, and the dissociation plots were constructed ***(68)*** (**Fig. 8**).

Repeated scanning of the same cells causes fluorescence fading. Unfortunately, the fading, which could be extensive when time intervals between scanning are short, imposes a limitation on the time resolution of the kinetic measurement. However, the fading rate as well as the fluorescence recovery rate can be measured in the same cells by LSC, and the results corrected appropriately ***(67)***.

9. LSC in Clinical Pathology

Cytometry still plays a relatively minor role in routine clinical pathology. However, by quantifying key attributes of selected cells in a specimen (tissue section or fine-needle aspirate [FNA]), cytometry can contribute useful prognostic information and help guide therapy. Because little cell loss occurs during sample preparation, LSC is particularly suitable for hypocellular specimens.

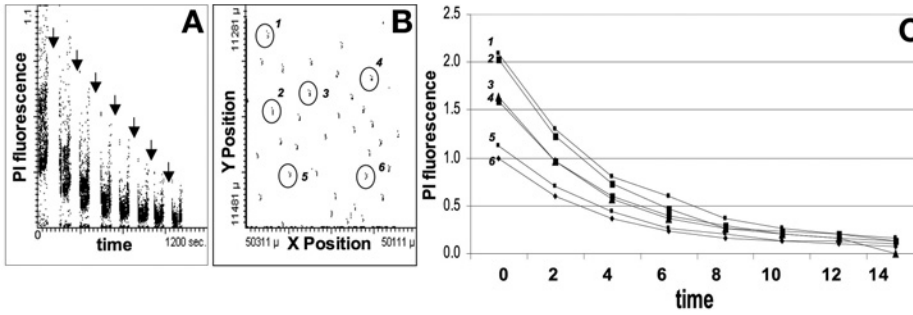

Fig. 8. Application of LSC in analysis of time resolved events; kinetics of removal of the DNA-bound PI from fixed cells by a solution containing caffeine. HL-60 cells attached to the microscope slide were treated with RNase and stained with PI. The cells were then repeatedly [arrows in **(A)**] rinsed with a 50-m*M* solution of caffeine in phosphate-buffered saline and cellular fluorescence was measured at different time-points. **(A)** The scattergram representing time vs PI (red) fluorescence intensity (integrated value) of the rinsed cells; **(B)** the *xy* spatial cell distribution on the slide. Because the same cells were analyzed repeatedly over time and the cell position was recorded in a list mode as one of the parameters, it was possible to select any cell, for example, based on its *xy* coordinates, and, by multiparameter analysis, obtain the kinetic curve for that cell. **(C)** Representative kinetic curves for six such cells marked (circles) in (B). Cells 1 and 2, having at 0 time twice the PI fluorescence intensity of cells 5 and 6, are most likely G_2/M cells; the latter are most likely G_1 cells. Caffeine removes PI from DNA by forming heterologous complexes with this dye in aqueous solutions, thereby altering equilibrium between bound and free PI, resulting in dissociation of the DNA–PI complexes *(68)*.

FNA samples *(69)*, sputum *(70)*, bladder washes *(71)*, neonatal blood samples *(46)*, and paraffin blocks *(72)* each provide an adequate number of cells/nuclei for analysis by LSC. LSC can also be used for analysis of histologic sections. Areas of interest that might be a minor component of the whole section can be selected to exclude extraneous tissues from measurement *(72)*. The specimens can be destained and restained *(68)* to measure additional attributes of the same cells; the relocation feature of LSC allows one to precisely identify each cell by its location on the slide. Several publications describe the usefulness of LSC in analysis of tissue sections, FNA samples, or touch preparations *(44,73–83)*.

One of the drawbacks inherent in measuring constituents of cells in histologic sections is that most of the cells are transected at different levels. Thus, because only a fraction of a cell or nucleus, unknown in size, is assayed, such measurement provides no information about the quantity of the measured constituent per cell. However, a ratiometric analysis, relating the quantity of the measured nuclear constituent per unit of DNA, normalizes the data and makes

them comparable between sections of different thicknesses *(80)*. Still to be worked out are the computer-assisted analytical methods that will be needed to fully exploit the information in histologic sections. In the case of solid tumors, this includes the relationship between tumor cells and reactive host cells, stroma, proliferating vessels, and so forth, the distribution of proliferating vs apoptotic cells within the tumor, the expression of growth factor receptors in tumor cells according to location and in relation to host cells and blood vessels, and the effect of drug therapies on the functional measurements of the cells. The number of measurable features is increasing, providing new tools to characterize and monitor human tumors in ways not possible by conventional light microscopy.

10. Utility of LSC in Other Applications

The major assets of LSC are the relocation and file-merge capabilities. These features are essential in studies of time-resolved events such as enzyme kinetics, transmembrane transport rates of drugs or metabolites, and other cell functions. Likewise, *in situ* association constants of fluorochrome-conjugated ligands with the respective receptors can easily be assessed for individual cells by LSC by repeatedly measuring ligand binding to the same cells as a function of increasing ligand concentrations. After archival preservation, the same cells can be subjected to further measurements with new probes and the results merged into a single file for multivariate analysis. The same cells can be sequentially studied—first when they are alive (e.g., surface immunophenotyped, subjected to functional assays for a particular organelle, oxidative metabolism, pH, enzyme kinetics, etc.) and then following their fixation (e.g., probed for DNA content to assess DNA ploidy and/or cell cycle distribution, DNA replication, content of an intracellular constituent[s] that can be detected immunocytochemically, etc.). To obtain their cytogenetic profile, cells can be subsequently probed by FISH or *in situ* polymerase chain reaction (PCR). The length of telomere sections of DNA can be conveniently estimated *in situ* by LSC using FISH telomere probes *(84,85)*. Conventional staining with absorption dyes followed by microscopy can further identify the measured cells and correlate their morphology with any of the measured parameters. If desired, a more sophisticated image analysis of the selected cells can follow. An attachment of LSC to the image analysis system (Kontron KS 100) through standard connections has been described *(86)*. The images collected by LSC can be digitally processed for further quantitative analysis *(31)*. LSC can also be combined with a laser-capture microdissection device to obtain histologically homogenous cell populations (e.g., for cytogenetic analysis) *(87)*.

Laser scanning cytometry has the potential to be used to analyze cell–cell interactions *in situ.* One such application, namely to detect platelet–endothelial

cell interactions, has already been demonstrated *(88)*. This assay can be a sensitive marker predictive of vascular thrombosis. We are currently testing the application of LSC to measure the kinetics of the in vitro "wound healing" in the model of mechanically or thermally damaged monolayer cultures of epithelial cells *(89)*.

Further applications might require more parameters to be measured. Sequential analyses of the same cells rely on the removal of the fluorescence from the earlier analyses prior to the next measurement. Currently available means of enzymatic or chemical removal of the fluorochrome *(59)*, or its bleaching, might not always be effective and new methods have to be developed. As mentioned, however, sequential measurements of the cells using the same color fluorescence but employing subtraction of the fluorescence signals to obtain differential fluorescence as a separate parameter *(64)* might circumvent, to some extent, a need for more colors. A violet laser, which is already available on new LSC models or can be retrofitted into old models, will further enhance LSC capability for multiparametric measurements with different color probes, alleviating the need for fluorochrome removal. New dye combinations provide additional possibilities to expand analytical capabilities of LSC for multiparameter cytometry *(90,91)*. Furthermore, a combination of fluorescence and time-delayed luminescence probes that are both color- and time- resolved *(92)* and can be adapted to LSC can double the analytical capability of this instrument.

The capability of spatial localization of a fluorochrome within the cell is another feature of LSC that is expected to attract new applications. LSC will also be used for the measurement of the translocation of different factors, such as components of the signal transduction pathway between cytoplasm and nucleus and between nucleolus and nucleoplasm, cytosol and mitochondria, organelle phenotyping, or transorganelle trafficking. LSC can also be used to measure a variety of attributes of live cells, including in vivo trafficking of any protein e.g., when fused with green fluorescent protein [GFP]), in cells cultured in a thermostated, optically transparent culture chamber mounted on the microscope stage.

Analysis of cell-to-cell interactions is another field in which LSC can find further applications. Signal transfer between the cells, cell-to-cell transport of the fluorochrome-tagged molecules, local differences in cell proliferative potential, and apoptosis can be studied on cells growing on slides, live and/or after fixation. Likewise, the role of cytokines or other growth factors released from individual cells on proliferation or apoptosis of the neighboring cells, whether in cell monolayers or in tissue sections, also can be studied by LSC.

By providing quantitative data on FNA, tissue sections, or cytology smears, LSC could also become widely used in clinical pathology. As new diagnostic and prognostic markers are rapidly being developed and their clinical utility

becomes more and more evident, the need for quantification of these markers is apparent.

Laser scanning cytometry has all of the required attributes, which, with relatively simple alterations, could be transformed into a three-modular instrument consisting of (1) a static cytometer, (2) a flow cytometer, and (3) a confocal microscope; that is, attachment of a module containing a flow channel to the microscope stage combined with immobilization of the laser beam transforms LSC into a flow cytometer. The existing scanning laser beam, on the other hand, when combined with pinhole apertures incorporated into an optical system of cell illumination and light collection, could transform LSC into a confocal microscope. Such a three-modular cytometer/confocal microscope could offer limitless analytical capabilities.

It was recently proposed that LSC might serve as both microscope and a cytometer in the *Space Station* ***(93)***, where it can be used for monitoring the crew's health and in ongoing biomedical experiments. Toward this end, the "liquidless" staining of specimens, which can be applicable at microgravity conditions, was developed ***(93)***. This futuristic application of LSC could be combined with automated or robotic handling of the specimen and data transmission to Earth.

11. Recent LSC Technology Developments

Since the submission of the original chapter two years ago, a new generation of laser scanning cytometers, the iGeneration instruments, has been released ***(94)***. Like the LSC, iGeneration instruments contain up to three lasers of different wavelengths, now enabling not only precise quantification of fluorescent signal but also laser light loss and imaging of cellular and tissue specimens on a solid substrate ***(94)***. Beams from the lasers are combined into a coincident path and directed to an inverted microscope (a new feature differentiating the iGeneration from the original technology) and onto a focal plane at the specimen.

The iGeneration's inverted format allows analysis of specimens on a variety of media, including microscope slides, microtiter plates, chamber slides, Petri dishes, or user-defined carriers fitting the footprint of a microtiter plate.

Autofocus is integral to iGeneration cytometers, minimizing operator involvement in the analysis. Although high-quality imaging on these systems eliminates the need for an optical microscope, it can still be provided to allow post-scan visualization of any location of interest. An optional robotic arm is also available for large-scale walk-away experiments, allowing automatic loading of up to 45 carriers.

The iGeneration software platform keeps much of the original LSC software functionality intact, as the LSC is considered the "gold standard" in solid-phase quantitative imaging cytometry. Raw scan data can be saved as JPEG or 16-bit

image files suitable for data processing, specimen visualization, and quantification by proprietary analytic software. Contours may be generated around cellular events based on the fluorescence intensity, forward scatter, or light absorption, either automatically to select an entire sample area, or user-defined to target specific types of events. Scan images may be assembled into tiled mosaic images, allowing contours to be drawn on tissue sections, cell colonies, and other large events that span multiple scan fields. Once the contours are generated, the software can perform a wide range of analyses and produce output in the form of numerical statistics, scattergrams, histograms, expression maps, or other statistical visualizations. Special mathematical operations allow correction for spectral overlap and tissue autofluorescence, and permit combining different time-lapse images. Analysis protocols are easily "written" by graphically assembling various functional modules to establish the desired analytical workflow. Each module's attributes can be easily modified, and the effect of these changes can be viewed immediately in the scanned images. Customizable protocol templates are provided as frameworks for different assays.

11.1. New Applications

The technology's performance characteristics make it suitable for a number of applications in basic life science research and drug discovery. Many new applications *(93)* are greatly facilitated by iGeneration's inverted format, expanded scatter and light-loss features, and enhanced cytometric analysis software. Space limitations allow only a few to be described.

Live-Cell Studies. iGeneration instruments allow live-cell analysis with minimal sample disruption. In many cases, multiple-dye homogenous staining cocktails can be used, eliminating specimen washing. This is particularly important in apoptosis applications, where fragile, loosely adherent apoptotic cells may be lost during washing, leading to potentially erroneous results. Cell-cycle analysis is performed simultaneously with other markers of plasma and nuclear membrane integrity for comprehensive evaluation of apoptotic pathways. Additionally, live cells can be analyzed and then fixed and restained with new reagents for further analysis. Live-cell toxicological analysis using a multiple-dye homogenous cocktail consisting of cell-cycle and apoptosis related markers is shown in **Fig. 9**. Among the notable drug effects are the abrogation of homotypic adhesion of the Jurkat cells **(Fig. 9A)**. An example of a scan field showing late apoptotic cells exhibiting red (propidium iodide) and green (annexin V staining) and early apoptotic cells hyperstained with Hoechst 33342 (DNA content) and expressing green annexin V are shown in **Fig. 9B**.

Automated Analysis of Tissues and Tissue Microarrays (TMAs). iGeneration platforms are well suited for analysis of samples with preserved tissue architecture, such as tissue imprints, TMAs, and tissue sections *(94–96)*.

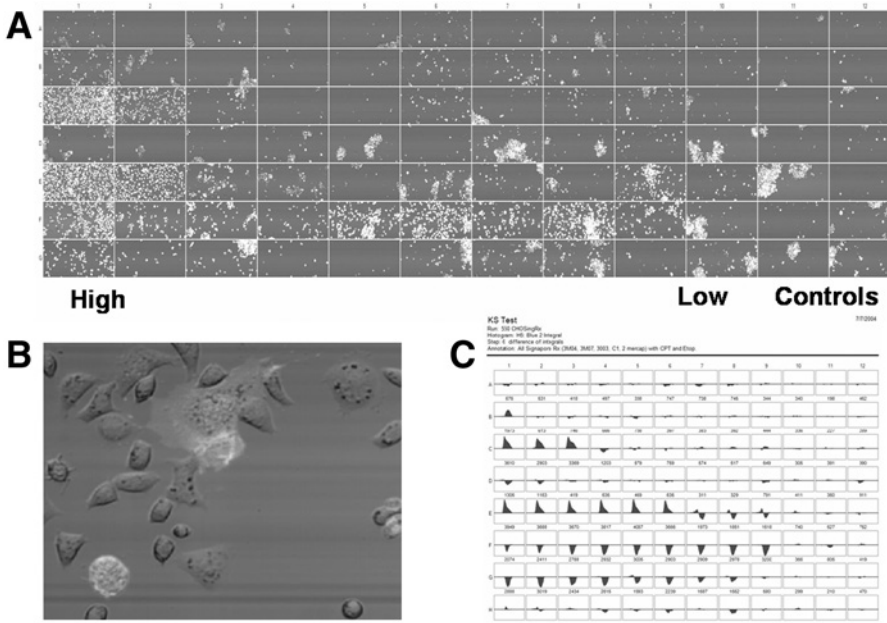

Fig. 9. Live-cell toxicological analysis using a multiple-dye homogenous cocktail. **(A)** Laser scan images of the Jurkat cells treated with a panel of mitochondrial-specific compounds and topoisomerase inhibitors camptothecin and etoposide. **(B)** Portion of a scan field showing early and late apoptotic cells. **(C)** Kolmogorov–Smirnov D-value histograms of DNA staining from adherent cells treated with the same test compounds.

New light-loss modes allow for simultaneous analysis of chromatically and fluorescently stained sections. Multi-scale scanning increases specimen throughput: an initial high-speed scan identifies specific objects or areas of interest for high-resolution re-scanning, which identifies their contents and quantifies constituents of interest. Unique image processing techniques correct for background fluorescence and spectral overlap of both fluorescent dyes and chromophores.

TMA analysis is emerging as the method of choice for biomarker discovery, and requires instrumentation capable of objective analysis and handling of multiple features measured on many tissue elements. An example shown in **Fig. 10** represents a prostate TMA labeled with CD10 developed with the chromophore DAB and counterstained with hematoxylin. Analysis employs blue and red laser light absorption to quantify DAB and hematoxylin, combined with detection of autofluorescence.

Research areas currently benefiting from LSC technology are system biology, early-stage drug discovery (particularly target identification, lead optimization, and predictive and investigative toxicology), biomarker discovery and

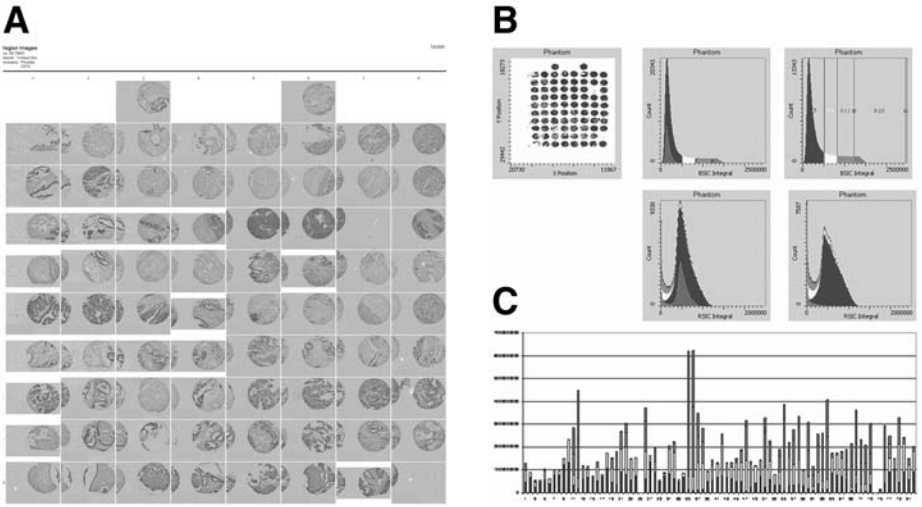

Fig. 10. Tissue microarray analysis of prostate TMA labeled with CD10 developed with the chromophore DAB and counterstained with hematoxylin. **(A)** Mosaic images of the individual core elements. DAB expression is color-coded red, hematoxylin is blue, and autofluorescence is green. **(B)** Quantitative analysis of the core elements using random sampling techniques. **(C)** CD10 expression of the individual elements of the TMA.

validation (with application in phase II and phase III clinical trials), immunophenotyping and immunohistochemistry analysis in clinical research.

Acknowledgments

This work was supported by NCI grant no. CA 28704 and the "This Close" Foundation for Cancer Research.

References

1. Kamentsky, L. A. and Kamentsky, L. D. (1991) Microscope-based multiparameter laser scanning cytometer yielding data comparable to flow cytometry data. *Cytometry* **12,** 81–87.
2. Kamentsky, L. A., Burger, D. E., Gershman, R. J., Kamentsky, L. D., and Luther, E. (1997) Slide-based laser scanning cytometry. *Acta Cytol.* **41,** 123–143.
3. Kamentsky, L. A. (2001) Laser scanning cytometry. *Methods Cell Biol.* **63,** 51–83.
4. Darzynkiewicz, Z., Bedner, E., Li, X., Gorczyca, W., and Melamed, M. R. (1999) Laser-scanning cytometry: a new instrumentation with many applications. *Exp. Cell Res.* **249,** 1–12.
5. Grabarek, J. and Darzynkiewicz, Z. (2002) Versatility of analytical capabilities of laser scanning cytometry (LSC). *Clin. Appl. Immunol. Rev.* **2,** 75–92.
6. Tarnok, A. and Gerstner, O. H. (2002) Clinical applications of laser scanning cytometry. *Cytometry* **50,** 133–143.

7. Roman, D., Greiner, B., Ibrahim, M., Pralet, D., and Germann, P. G. (2002) Laser technologies in toxipathology. *Toxicol. Pathol.* **30,** 11–14.
8. Taatjes, D. J., Palmer, C., Pantano, C., Hoffmann, S. B., Cummins, A., and Mossman, B. T. (2001) Laser-based microscopic approaches: application to cell signaling in environmental lung disease. *Biotechniques* **31,** 880–894.
9. Luther, E. and Kamentsky, L. A. (1996) Resolution of mitotic cells using laser scanning cytometry. *Cytometry* **23,** 272–278.
10. Kawasaki, M., Sasaki, K., Satoh, T., et al. (1997) Laser scanning cytometry (LSC) allows detailed analysis of the cell cycle in PI stained human fibroblasts (TIG-7). *Cell Prolif.* **30,** 139–147.
11. Juan, G., Traganos, F., James, W. M., et al. (1998) Histone H3 phosphorylation and expression of cyclins A and B1 measured in individual cells during their progression through G_2 and mitosis. *Cytometry* **21,** 1–8.
12. Gorczyca, W., Melamed, M. R., and Darzynkiewicz, Z. (1996) Laser scanning cytometer (LSC) analysis of fraction of labeled mitoses (FLM). *Cell Prolif.* **29,** 9–47.
13. Quastler, H. and Sherman, F. G. (1959) Cell population kinetics in the intestinal epithelium of mouse. *Exp. Cell Res.* **24,** 420–438.
14. Schmid, T. E., Attia, S., Baumargartner, A., Nuesse, M., and Adler, I. D. (2001) Effect of chemicals on the duration of male meiosis in mice detected with laser scanning cytometry. *Mutagenesis* **16,** 339–343.
15. Darzynkiewicz, Z., Juan, G., Li, X., Gorczyca, W., Murakami, T., and Traganos, F. (1997) Cytometry in cell necrobiology: Analysis of apoptosis and accidental cell death (necrosis). *Cytometry* **27,** 1–20.
16. Darzynkiewicz, Z., Bruno, S., Del Bino, G., et al. (1992) Features of apoptotic cells measured by flow cytometry. *Cytometry* **13,** 795–808.
17. Furuya, T., Kamada, T., Murakami, T., Kurose, A., and Sasaki, K. (1997) Laser scanning cytometry allows detection of cell death with morphological features of apoptosis in cells stained with PI. *Cytometry* **29,** 173–177.
18. Bedner, E., Li, X., Gorczyca, W., Melamed, M. R., and Darzynkiewicz, Z. (1999) Analysis of apoptosis by laser scanning cytometry. *Cytometry* **35,** 181–195.
19. Telford, W. G., Komoriya, A., and Packard, B. Z. (2002) Detection of localized caspase activity in early apoptotic cells by laser scanning cytometry. *Cytometry* **47,** 81–88.
20. Bedner, E., Burfeind, P., Gorczyca, W., Melamed, M. R., and Darzynkiewicz, Z. (1997) Laser scanning cytometry distinguishes lymphocytes, monocytes and granulocytes by differences in their chromatin structure. *Cytometry* **29,** 191–196.
21. Wolter, K. G., Hsu, I. T., Smith, C. L., Hechusthan, A., Xi, X. G., and Youle, R. J. (1997) Movement of *Bax* from the cytosol to mitochondria during apoptosis. *J. Cell Biol.* **139,** 1281–1292.
22. Zamzani, N., Brenner, C., Marzo, I., Susin, S. A., and Kroemer, G. (1998) Subcellular and submitochondrial mode of action of *Bcl-2*-like oncoproteins. *Oncogene* **16,** 2265–2282.
23. Bedner, E., Li, X., Kunicki, J., and Darzynkiewicz, Z. (2000) Translocation of *Bax* to mitochondria during apoptosis measured by laser scanning cytometry. *Cytometry* **41,** 83–88.

24. Baldwin, A. S., Jr. (1996) The NF-κB and IκB proteins: new discoveries and insights. *Annu. Rev. Immunol.* **14,** 649–681.
25. Deptala, A., Bedner, E., Gorczyca, W., and Darzynkiewicz, Z. (1998) Activation of nuclear factor kappa B (NF-κB) assayed by laser scanning cytometry (LSC). *Cytometry* **33,** 376–382.
26. Mercie, P., Belloc, F., Biblou-Nabera, C., et al. (2000) Comparative methodologic study on NFκB activation in cultured endothelial cells. *J. Lab. Clin. Med.* **136,** 402–411.
27. Deptala, A., Li, X., Bedner, E., Cheng, W., Traganos, F., and Darzynkiewicz, Z. (1999) Differences in induction of p53, $p21^{WAF1}$, and apoptosis in relation to cell cycle phase of MCF-7 cells treated with camptothecin. *Int. J. Oncol.* **15,** 861–871.
28. Kawamura, K., Kobayashi, Y., Tanaka, T., Ikeda, R., Fujikawa-Yamamoto, K., and Suzuki, K. (2002) Intranuclear localization of proliferating cell nuclear antigen during the cell cycle in renal cell carcinoma. *Anal. Quant. Cytol. Histol.* **22,** 107–113.
29. Styles, J. A., Clark, H., Festing, M. F. W., and Rew, D. A. (2001) Automation of mouse micronucleus genotoxicity assay by laser scanning cytometry. *Cytometry* **44,** 153–155.
30. Smolewski, P., Ruan, Q., Vellon, L., and Darzynkiewicz, Z. (2001) The micronuclei assay by laser scanning cytometry. *Cytometry* **45,** 19–26.
31. Petersen, A. B., Gniadecki, R., and Wulf, H. C. (2000) Laser scanning cytometry for comet assay analysis. *Cytometry* **39,** 10–15.
32. Bacso, Z. and Eliason, J. F. (2001) Measurement of DNA damage associated with apoptosis by laser scanning cytometry. *Cytometry* **45,** 180–186.
33. Kamentsky, L. A., Kamentsky, L. D., Fletcher, J. A., Kurose, A., and Sasaki, K. (1997) Methods for automatic multiparameter analysis of fluorescence *in situ* hybridized specimens with laser scanning cytometer. *Cytometry* **27,** 117–125.
34. Kobayashi, Y., Yesato, K., Oga, A., and Sasaki, K. (2002) Detection of 20q13 gain by dual-color FISH in breast cancers. *Anticancer Res.* **20,** 531–535.
35. Hashimoto, Y., Oga, A., Okami, K., Imate, Y., Yamashita, Y., and Sasaki, K. (2002) Relationship between cytogenetic aberrations by CGH coupled with tissue microdissection and DNA ploidy by laser scanning cytometry in head and neck squamous cell carcinoma. *Cytometry* **40,** 161–166.
36. Harada, K., Nishizaki, T., Ozaki, S., et al. (1999) Cytogenetic alteration in pituitary adenomas detected by comparative genomic hybridization. *Cancer Genet. Cytogenet.* **112,** 38–41.
37. Harada, K., Nishizaki, T., Kubota, H., Harada, K., Suzuki, M., and Sasaki, K. (2001) Distinct primary central nervous system lymphoma defined by comparative genomic hybridization and laser scanning cytometry. *Cancer Genet. Cytogenet.* **125,** 147–150.
38. Baumgartner, A., Schmid, T. E., Maers, H. K., Adler, I. D., Tarnok, A., and Nuesse, M. (2001) Automated evaluation of frequencies of aneuploid sperm by laser-scanning cytometry (LSC). *Cytometry* **44,** 156–160.
39. Juan, G. and Cordon-Cardo, C. (2001) Intranuclear compartmentalization of cyclin E during the cell cycle: disruption of the nucleoplasm–nucleolar shuttling of cyclin E in bladder cancer. *Cancer Res.* **61,** 1220–1226.

40. Gorczyca, W., Smolewski, P., Ardelt, B., Ita, M., Melamed, M. R., and Darzynkiewicz, Z. (2001) Morphometry of nucleoli and expression of nucleolin analyzed by laser scanning cytometry in mitogenically stimulated lymphocytes. *Cytometry* **45,** 206–213.
41. Bedner, E., Ruan, Q., Chen, S., Kamentsky, L. A., and Darzynkiewicz, Z. (2000) Multiparameter analysis of progeny of individual cells by laser scanning cytometry. *Cytometry* **40,** 271–279.
42. Clatch, R. J., Foreman, J. R., and Walloch, J. L. (1998) Simplified immunophenotypic analysis by laser scanning cytometry. *Cytometry* **34,** 3–16.
43. Clatch, R. J. and Foreman, J. R. (1998) Five-color immunophenotyping plus DNA content analysis by laser scanning cytometry. *Cytometry* **34,** 36–38.
44. Clatch, R. J. and Walloch, J. L. (1997) Multiparameter immunophenotypic analysis of fine needle aspiration biopsies and other hematologic specimens by laser scanning cytometry. *Acta Cytol.* **41,** 109–122.
45. Clatch, R. J. (2001) Immunophenotyping of hematological malignancies by laser scanning cytometry. *Methods Cell Biol.* **64,** 313–342.
46. Gerstner, A., Lafler, W., Bootz, F., and Tarnok, A. (2000) Immunophenotyping of peripheral blood by laser scanning cytometry. *J. Immunol. Methods.* **246,** 175–185.
47. Kerr, J. F. R., Wyllie, A. H., and Curie, A. R. (1972) Apoptosis: a basic biological phenomenon with a wide-ranging implications in tissue kinetics. *Br. J. Cancer* **26,** 239–257.
48. Bedner, E., Halicka, H.D., Cheng, W., et al. (1999) High affinity binding of fluorescein isothiocyanate to eosinophils detected by laser scanning cytometry: a potential source of error in analysis of blood samples utilizing fluorescein conjugated reagents in flow cytometry, *Cytometry* **36,** 77–82.
49. Bedner, E., Burfeind, P., Hsieh, T.-C., et al. (1998) Cell cycle effects and induction of apoptosis caused by infection of HL-60 cells with human granulocytic ehrlichiosis (HGE) pathogen measured by flow and laser scanning cytometry (LSC). *Cytometry* **33,** 47–55.
50. Darzynkiewicz, Z., Bedner, E., Traganos, F., and Murakami, T. (1998) Critical aspects in the analysis of apoptosis and necrosis. *Hum. Cell* **11,** 3–12.
51. Darzynkiewicz, Z., Bedner, E., and Traganos, F. (2001) Difficulties and pitfalls in analysis of apoptosis. *Methods Cell Biol.* **63,** 527–546.
52. Li, X., Melamed, M. R., and Darzynkiewicz, Z. (1996) Detection of apoptosis and DNA replication by differential labeling of DNA strand breaks with fluorochromes of different color. *Exp. Cell Res.* **222,** 28–37.
53. Darzynkiewicz, Z. and Bedner, E. (2000) Analysis of apoptotic cells by flow- and laser scanning- cytometry. *Methods Enzymol.* **322,** 18–39.
54. Darzynkiewicz, Z., Bedner, E., Burfeind, P., and Traganos, F. (1998) Analysis of apoptosis by flow and laser scanning cytometry, in *Apoptosis. Detection and Assay Methods* (Zhu L. and Chun J., eds.), BioTechniques Books Series, Eaton, Natick, MA, pp. 75–92.
55. Gorczyca, W., Bedner, E., Burfeind, P., Darzynkiewicz, Z., and Melamed, M. R. (1998) Analysis of apoptosis by laser-scanning cytometry. *Mod. Pathol.* **11,** 1052–1058.

56. Abdel-Moneim, L., Melamed, M. R., Darzynkiewicz, Z., and Gorczyca, W. (2000) Proliferation and apoptosis in solid tumors. Analysis by laser scanning cytometry. *Anal. Quant. Cytol. Histol.* **22,** 393–397.
57. Zabaglo, L., Ormerod, M. G., and Dowsett, M. (2000) Measurement of markers for breast cancer in model system using laser scanning cytometry. *Cytometry* **41,** 166–171.
58. Darzynkiewicz, Z., Li, X., and Bedner, E. (2001) Use of flow and laser-scanning cytometry in analysis of cell death. *Methods Cell Biol.* **66,** 69–109.
59. Bedner, E., Smolewski, P., Amstad, P., and Darzynkiewicz, Z. (2000) Activation of caspases measured in situ by binding of fluorochrome-labeled inhibitors of caspases (FLICA: correlation with DNA fragmentation. *Exp. Cell Res.* **259,** 308–315.
60. Smolewski, P., Bedner, E., Du, L., et al. (2001) Detection of caspases activation by fluorochrome-labeled inhibitors: multiparameter analysis by laser scanning cytometry. *Cytometry* **44,** 73–82.
61. Grabarek, J., Dragan, M., Lee, B. W., Johnson, G. L., and Darzynkiewicz, Z. (2002) Activation of chymotrypsin-like protease(s) during apoptosi detected by affinity-labeling of the enzymatic center with fluoresceinated inhibitor. *Int. J. Oncol.* **20,** 225–233.
62. Halicka, H. D., Bedner, A., and Darzynkiewicz, Z. (2000) Segregation of RNA and separate packaging of DNA and RNA in apoptotic bodies during apoptosis. *Exp. Cell Res.* **260,** 248–256.
63. Kakino, S., Sasaki, K., Kurose, A., and Ito, H. (1996) Intracellular localization of cyclin B1 during cell cycle in gliomas cells. *Cytometry* **24,** 49–54.
64. Smolewski, P., Grabarek, J., Kamentsky, L. A., and Darzynkiewicz, Z. (2001) Bivariate analysis of cellular DNA versus RNA content by laser scanning cytometry using the product of signal subtraction (Differential Fluorescence) as a separate parameter. *Cytometry* **45,** 73–78.
65. Li, X. and Darzynkiewicz, Z. (1999) The Schrödinger's cat quandary in biology: integration of live cell functional assays with measurements of fixed cells in analysis of apoptosis. *Exp.Cell Res.* **249,** 404–412.
66. Li, X., Du, L., and Darzynkiewicz, Z. (2000) During apoptosis of HL-60 and U-937 cells caspases are activated independently of dissipation of mitochondrial electrochemical potential. *Exp. Cell Res.* **257,** 290–297.
67. Bedner, E., Melamed, M. R., and Darzynkiewicz, Z. (1998) Enzyme kinetic reactions and fluorochrome uptake rates measured in individual cells by laser scanning cytometry (LSC). *Cytometry* **33,** 1–9.
68. Bedner, E., Du, L., Traganos, F., and Darzynkiewicz, Z. (2001) Caffeine dissociates complexes between DNA and intercalating dyes: Application for bleaching fluorochrome-stained cells for their subsequent restaining and analysis by laser scanning cytometry. *Cytometry* **43,** 38–45.
69. Clatch, R. J., Walloch, J. L., Foreman, J. R., and Kamentsky, L. A. (1997) Multiparameter analysis of DNA content and cytokeratin expression in breast carcinoma by laser scanning cytometry. *Arch. Pathol. Lab. Med.* **121,** 585–592.
70. Woltmann, G., Ward, R. J., Symon, F. A., Rew, D. A., Pavord, I. D., and Wardlaw, A. J. (1999) Objective quantitative analysis of eosinophils and

bronchial epithelial cells in induced sputum by laser scanning cytometry. *Thorax* **54,** 124–130.
71. Wojcik, E. M., Saraga, S. A., Jin, J. K., and Hendricks, J. B. (2001) Application of laser scanning cytometry for evaluation of DNA ploidy in routine cytologic specimens. *Diagn. Cytopathol.* **24,** 200–205.
72. Kamiya, N., Yokose, T., Kiyomatsu, Y., Fahey, M. T., Kodama, T., and Mukai, K. (1999) Assessment of DNA content in formalin-fixed, paraffin-embeded tissue of lung cancer by laser scanning cytometry. *Pathol. Int.* **49,** 695–701.
73. Grace, M. J., Xie, L., Musco, M. L., et al. (1999) The use of laser scanning cytometry to assess depth of penetration of adenovirus p53 gene therapy in human xenograft biopsies. *Am. J. Pathol.* **155,** 1869–1878.
74. Musco, M. L., Shijun, C., Small, D., Nodelman, M., Sugarman, B., and Grace, M. (1998) Comparison of flow cytometry and laser scanning cytometry for the intracellular evaluation of adenoviral infectivity and p53 protein expression in gene therapy. *Cytometry* **33,** 290–296.
75. Rew, D. A., Reeve, L. J., and Wilson, G. D. (1998) Comparison of flow and laser scanning cytometry for the assay of cell proliferation in human solid tumors. *Cytometry* **33,** 355–361.
76. Gorczyca, W., Darzynkiewicz, Z., and Melamed, M. R. (1997) Laser scanning cytometry in pathology of solid tumors. A review. *Acta Cytol.* **41,** 98–108.
77. Gorczyca, W., Sarode, V., Melamed, M. R., and Darzynkiewicz, Z. (1997) Laser scanning cytometric analysis of cyclin B1 in primary human malignancies. *Mod. Pathol.* **10,** 457–462.
78. Kawamura, K., Tanaka, T., Ikeda, R., Fujikawa-Yamamoto, K., and Suzuki, K. (2000) DNA ploidy analysis in urinary tract epithelial tumors by laser scanning cytometry. *Anal. Quant. Cytol. Histol.* **22,** 26–30.
79. Gorczyca, W., Bedner, E., Burfeind, P., Darzynkiewicz, Z., and Melamed, M. R. (1998) Analysis of apoptosis in solid tumors by laser scanning cytometry. *Mod. Pathol.* **11,** 1–7.
80. Gorczyca, W., Davidian, M., Gherson, J., Ashikari, R., Darzynkiewicz, Z., and Melamed, M. R. (1999) Laser scanning cytometry quantification of estrogen receptors in breast cancer. *Anal. Quant. Cytol. Histol.* **20,** 470–476.
81. Tsukazaki, Y., Numa, Y., Zhao, S., and Kawamoto, K. (2000) Analysis of DNA-ploidy using laser scanning cytometer in brain tumors and its clinical application. *Hum. Cell* **13,** 221–228.
82. Gerstner, A. O., Machlitt, J., Laffers, W., Tarnok, A., and Bootz, F. (2002) Analysis of minimal sample volumes from head and neck cancer by laser scanning cytometry. *Onkologie* **25,** 40–46.
83. Bollman, R., Torks, R., Schmitz, J., Bolman, M., and Mehes, G. (2002) Determination of ploidy and steroid receptor status in breast cancer by laser scanning cytometry. *Cytometry* **50,** 210–215.
84. Kajstura, J., Peroldi, B., Leri, A., et al. (2000) Telomere shortening is an *in vivo* marker of myocyte replication and aging. *Am. J. Pathol.* **156,** 813–819.
85. Izumi, H., Hara, T., Oga, A., et al. (2002) High telomerase activity correlates with the stabilities of genome and DNA ploidy in renal carcinoma. *Neoplasia* **4,** 103–111.

86. Woltmann, G., Wardlaw, A. J., and Rew, D. A. (1997) Image analysis enhancement of the laser scanning cytometer. *Cytometry* **33,** 262–265.
87. Mora, J., Cheung, N. K., Juan, G., et al. (2001) Neuroblastic and Schwannian stromal cells of neuroblastoma are derived from a tumor progenitor cell. *Cancer Res.* **61,** 6892–6898.
88. Claytor, R. B., Li, J. M., Furman, M. I., et al. (2001) Laser scanning cytometry: a novel method for the detection of platelet-endothelial cell adhesion. *Cytometry* **43,** 308–313.
89. Haider, A. S., Grabarek, J., Eng, B., et al. (2003) In vitro wound healing analyzed by laser scanning cytometry. Accelerated healing of epithelial cell monolayers in the presence of hyaluronate. *Cytometry* **53A,** 1–8.
90. Police, A. A., Smith, C. A., Brown, K., Farkas, D. L., Silverman, J. F., and Shackney, S. E. (2002) Multiparameter analysis of human epithelial tumor cell lines by laser scanning cytometry. *Cytometry* **42,** 347–356.
91. Gerstner, A. O., Lenz, D., Laffers, W., et al. (2002) Near-infrared dyes for six-color immunophenotyping by laser scanning cytometry. *Cytometry* **48,** 115–125.
92. Tanke, H. J., De Haas, R. R., Sagner, G., Ganser, M., and van Gijlswijk, R. P. M. (1998) Use of platinum coproporphyrin and delayed luminescence imaging to extend the number of targets FISH karyotyping. *Cytometry* **33,** 453–459.
93. Smolewski, P., Bedner, E., Gorczyca, W., and Darzynkiewicz, Z. (2001) "Liquidless" cell staining by dye diffusion from gels and analysis by laser scanning cytometry: potential application at microgravity conditions in space. *Cytometry* **44,** 355–360.
94. Luther, E., Kamentsky, L., Henriksen, M., and Holden, E. (2004) Next-generation laser scanning cytometry. *Methods Cell Biol.* **75,** 185–218.
95. Megyeri, A., Bacso, *Z.,* Shields, A., and Eliason. J. (2005) Development of a stereological method to measure levels of fluoropyrimidine metabolizing enzymes in tumor sections using laser scanning cytometry. *Cytometry A* **64,** 62–71.
96. Pruimboom-Brees, I., et al. (2005) Using laser scanning cytometry to measure PPAR-mediated peroxisome proliferation and oxidation. *Tox. Path.* **33,** 86–91.
97. Davis, D., Takamori, R., Raut, C. P., et al. (2005) Pharmacodynamic analysis of target inhibition and endothelial cell death in tumors treated with the vascular endothelial growth factor receptor antagonists SU5416 and SU6668. *Clin. Cancer Res.* **11,** 678–689.